Cactin is essential for G1 progression in Toxoplasma gondii

Citation: Szatanek, Tomasz et al. "Cactin Is Essential for G1 Progression in Toxoplasma Gondii: Cactin Is Essential for Toxoplasma G1 Progression." Molecular Microbiology 84.3 (2012): 566–577.

As Published: http://dx.doi.org/10.1111/j.1365-2958.2012.08044.x

Publisher: Wiley Blackwell

Persistent URL: http://hdl.handle.net/1721.1/85629

Version: Author's final manuscript: final author's manuscript post peer review, without publisher's formatting or copy editing

Published in final edited form as:
Mol Microbiol. 2012 May ; 84(3): 566–577. doi:10.1111/j.1365-2958.2012.08044.x.

Cactin is essential for G1 progression in *Toxoplasma gondii*

Tomasz Szatanek[1], **Brooke R. Anderson-White**[1], **David M. Faugno-Fusci**[1], **Michael White**[2], **Jeroen P.J. Saeij**[3], and **Marc-Jan Gubbels**[1,*]

[1]Department of Biology, Boston College, Chestnut Hill, MA 02467, USA

[2]Departments of Molecular Medicine & Global Health, Florida Center for Drug Discovery and Innovation, Colleges of Medicine & Public Health, University of South Florida, Tampa, FL 33612, USA

[3]Department of Biology, Massachusetts Institute of Technology, Cambridge, MA 02139, USA

Abstract

Toxoplasma gondii is an obligate intracellular protozoan parasite whose rapid lytic replication cycles define its pathogenicity. We identified a temperature sensitive growth mutant, FV-P6, which irreversibly arrests before the middle of the G1 stage of the tachyzoite cell cycle. This arrest is caused by a point mutation in a gene conserved across eukaryotes, *Cactin*, whose product localizes to the nucleus. To elucidate the role of TgCactin we performed genome-wide expression profiling. Besides the expected G1 expression profile, many genes associated with the extracellular state as well as with the bradyzoite cyst stage were identified. Consistent with these profiles were the expression of AP2 transcription factors typically associated with extracellular and bradyzoite stage parasites. This suggests a role for TgCactin in control of gene expression. Since TgCactin does not contain any functionally defined domains we reasoned TgCactin exerts its function through interactions with other proteins. In support of this model we demonstrated that TgCactin is present in a protein complex and can oligomerize. Taken together, these results suggest that TgCactin acts as a pivotal protein potentially regulating gene expression at several transition points in parasite development.

Keywords

Toxoplasma; Cactin; cell cycle; G1; AP2

Introduction

The pathogenesis of diseases caused by apicomplexan parasites is largely based on lytic intracellular replication cycles causing extensive tissue damage. Members of this phylum include the human pathogens *Toxoplasma gondii*, which causes encephalitis and birth defects (Montoya & Liesenfeld, 2004), *Plasmodium* species (spp.) that cause malaria (Haldar & Mohandas, 2009), and opportunistic infections such as *Cryptosporidium* spp. that cause acute gastroenteritis (Tzipori & Ward, 2002). In addition, apicomplexan parasites contribute to significant economic losses in the veterinary industry with *Eimeria* spp., infecting poultry and cattle (Shirley *et al.*, 2005), and *Theileria* and *Babesia* spp. infecting various ruminants (Mehlhorn & Shein, 1984). It has been noted that the parasite growth rate correlates with virulence and in general is a dominant factor in apicomplexan pathogenicity (Gubbels *et al.*, 2008b, Reilly *et al.*, 2007). Specifically, in *Toxoplasma* it has been shown

*To whom correspondence should be addressed. gubbelsj@bc.edu.

The authors declare no conflict of interest.

that the length of the G1 phase of the cell cycle is shortened in more virulent genotype I strains (Radke *et al.*, 2001); therefore, factors enhancing cell cycle progression through G1 are potential virulence factors and are potential targets to attenuate pathogenesis. A reversible pharmacological block of G1 progression using pyrrolidine dithiocarbamate (PDTC) has provided direct evidence for a G1 checkpoint (Conde de Felipe *et al.*, 2008), whereas a natural G0 arrest is present in extracellular parasites (Lescault *et al.*, 2010, Gaji et al., 2011). Here we report on the characterization of a conserved protein, Cactin, and its role in the G1 stage of the *Toxoplasma* cell cycle.

A forward genetic screen for temperature sensitive (*ts*) growth defects identified mutant FV-P6, which arrested in G1 (Gubbels *et al.*, 2008a). In this mutant a point mutation in the *Cactin* gene was shown to be responsible for the growth arrest. Although Cactin was identified in *Drosophila* over a decade ago (Lin *et al.*, 2000), its role and function in eukaryotes is still poorly understood despite its strong conservation throughout the eukaryotic lineage. Its initial description suggested a role in the Rel pathway of transcriptional control, but since then orthologs have been discovered in sequenced genomes of many organisms without a Rel pathway. In such organisms the role of Cactin is elusive. To elucidate the role of TgCactin in G1 arrest of *Toxoplasma,* which lacks the Rel pathway, we performed genome-wide expression profiling on the arrested mutant. This revealed a G1 expression profile in the arrested mutant along with many genes associated with the extracellular state as well as the bradyzoite tissue cyst stage. These data suggest a role for TgCactin in the control of gene expression at various points in parasite development. Notably, the G1, extracellular, and bradyzoite gene expression profiles were consistent with the increased expression levels of various Apetala2 (AP2) transcription factors associated with these stages. We further demonstrated that TgCactin is present in a complex and can oligomerize. Taken together, these results show that TgCactin is required for both G1 progression and state/stage transitions. This is reflected in the AP2 transcription factor expression pattern.

Results

Temperature sensitive mutant FV-P6 arrests in the middle of G1

Temperature sensitive mutant FV-P6 was identified in a large-scale screen for *T. gondii* tachyzoite growth mutants (Gubbels et al., 2008a). At the restrictive temperature of 40°C mutant FV-P6 displays an arrest in G1, which was defined by DNA content analysis. To characterize this defect in further detail we first analyzed the G1 arrest with cell biological markers for both the centrosome and internal daughter budding (α-Centrin and α-IMC3 antibodies, respectively). Using these markers three, different populations can be discerned in wild type parasites: 1 centrosome and no daughter buds (1C0B), 2 centrosomes and no daughter buds (2C0B), and 2 centrosomes with 2 daughter buds (2C2B) (Fig. 1A). The centrosomes duplicate late in G1 before the onset of S-phase whereas IMC3 containing daughter buds start developing at the onset of mitosis when DNA replication is about 90% complete (1.8N) (Anderson-White *et al.*, 2011, Nishi *et al.*, 2008, Radke et al., 2001). To establish the kinetics of the arrest we counted the distribution of the three morphologies every 3 hours over an 18-hour period. Before placing the parasites at 40°C (t = 0 hrs) they were allowed to replicate for 18 hrs at 35°C a time point whereat they are considered completely unsynchronized (Behnke *et al.*, 2010, Radke et al., 2001). As shown in Figure 1A, upon transition to 40°C the first round of cell division (~7 hrs) is representative of an unsynchronized population containing approximately 60% 1C0B, 30% 2C0B and 10% 2C2B parasites. In the next 9 hrs, roughly corresponding to an additional cell division cycle, the population arrests at nearly 100% 1C0B parasites. This corresponds with the DNA content analysis (Gubbels et al., 2008a) and confirms an arrest in the G1 stage of the cell cycle. No structural or morphological defects were observed with the markers used.

Recently, we described a family of intermediate filament-like IMC proteins with distinct spatiotemporal dynamics throughout the cell cycle (Anderson-White et al., 2011). Three of the IMC proteins, IMC7, 12 and 14, change their localization from the cytoplasm to the cortical cytoskeleton within G1. The IMC14 mRNA expression profile throughout tachyzoite development peaks very early in G1. This is before the peaks in the profiles of IMC7 and 12, which occur in the middle of G1. We confirmed these profiles at the protein level using a fluorescent reporter line of IMC14 in combination with a specific anti serum against IMC7 (Fig. S1A). Using red fluorescent protein reporters of IMC7 and IMC14 in mutant FV-P6, we determined in which stage of G1 its arrest occurs (Fig. 1B). In addition, in this experiment we tested whether the G1 arrest of FV-P6 was identical for parasites coming out of S-phase (initially dividing at 35°C; Fig. 1C), and for parasites coming out of G0 (direct invasion at 40°C; Fig. 1D). We observed that under both conditions tested, IMC7 is distributed 50:50 between a cortical and a cytoplasmic population, whereas IMC14 is 100% cortical at 40°C, regardless of the previous cell cycle stage (Fig. 1C,D). To define the base line we also determined the localization of IMC7 and IMC14 in G0 extracellular parasites. For IMC7 around 50% of the parasites displayed cortical localization, whereas only 10% of the population displayed cortical IMC14 (Fig. S1B–D). The distribution patterns in FV-P6 therefore indicate that the G1 arrest is after IMC14 transitions to the cortex but before IMC7 completes its transition to the cortex. Taken together, we can conclude that FV-P6 arrests after IMC14 transitions to the cortex and before duplication of the centrosomes. This timing is right before or in the middle of G1 progression.

Mutant FV-P6 G1 arrest is not reversible

The above data indicates that the parasites arrest in the middle of G1. The next question we asked is whether this arrest is reversible, which would be an indicator of the type of defect induced in the mutant. To investigate the reversibility of FV-P6 we took a phenotype reversion approach with plaque assays as the read-out. We measured reversion potency by letting FV-P6 parasites form plaques at 35°C after various exposure protocols at 40°C (Fig. 1E and F). Exposure of mutant as well as wild-type parasites freshly harvested at 35°C in their extracellular stage at 40°C results in a rapid loss of viability for both the mutant and wild-type lines (Fig. 1E). However, when parasites are allowed to invade and replicate at 40°C the plaque forming capacity of mutant FV-P6 rapidly drops whereas the parent line maintained full plaque forming capability (Fig. 1F). As shown in Figure 1E, this change is not due to a differential loss of viability of extracellular parasites at 40°C. Since the phenotype induction data in Figure 1A show that the arrest begins after 9 hrs, this indicates the parasites are not already dead at the first 8 hr time point in this reversion experiment. Therefore we conclude that the G1 arrest of mutant FV-P6 is not reversible.

The Cactin gene contains the etiological mutation

The gene containing the etiological point mutation in FV-P6 was previously shown to encode a Cactin ortholog (ToxoDB ID: TGME49_044380) by genetic complementation with a wild type cosmid library (Gubbels et al., 2008a). We validated this result by demonstrating that the *Cactin* allele found in FV-P6 is unable to complement the phenotype. Upon FV-P6 transfection of the PCR amplified *Cactin* allele from wild type genomic DNA plaques do form at 40°C (Fig. S2A, top panel). In contrast, no plaques form upon transfection of the *Cactin* allele PCR amplified from FV-P6 genomic DNA (Fig. S2A, bottom panel). In addition we assessed phenotype restoration using the Centrin/IMC3 assay as described in Figure 1A. Using this assay, we were unable to detect any significant difference between wild type parasites and FV-P6 parasites complemented with the wild-type *Cactin* amplicon grown at either 35°C or 40°C (Fig. S2B). Therefore, a mutation in the *Cactin* gene must be the sole cause of the G1 arrest.

Cactin is a conserved protein localizing to the nucleus

We determined the nature of the Cactin mutation by sequencing the wild-type allele and the FV-P6 allele. A single T to C point mutation resulting in an amino acid change from tyrosine to histidine (Y661H) was detected ((Gubbels et al., 2008a) and Fig. 2A). This residue is contained in the C-terminus and database searches identified this domain as strongly conserved across Cactin orthologs in other eukaryotes (Fig. 2A,B). Phylogenetic analysis of the *Cactin* gene indicates that it is ancient to the eukaryotic lineage, as it generally follows the accepted relationship patterns across the eukaryotes (Fig. 2C). Although Cactin was identified in *Drosophila* over a decade ago (Lin *et al.*, 2000) its role and function in eukaryotes is still poorly understood. Its initial description suggested a role in the Rel pathway of transcriptional control, but orthologs have since been discovered in sequenced genomes of many organisms that lack a Rel pathway. In such organisms, including *Saccharomyces pombe*, *Arabidopsis thaliana*, and *T. gondii* the role of Cactin is not understood.

Further sequence analysis identified a nuclear localization signal (NLS) at the N-terminus (amino acids 3–7: KKRRK) as well as an internal Robbins and Dingwall NLS (Robbins *et al.*, 1991) at amino acid position 499–515 (RRANLKKTLIQKERLKR) (Fig. 2B). With this in mind we expressed a YFP-tagged Cactin construct in the parasites that co-localizes in the nucleus with a Histone H2b-mRFP construct (Fig. 2D,E). Notably, TgCactin is present in the nucleus throughout the entire tachyzoite cell cycle. The Y661H *ts* allele of TgCactin also localized to the nucleus with no differences between 35°C and 40°C, which is expected since the NLS signals are not mutated (not shown).

Genome-wide expression profiling identifies a unique expression pattern

Since Cactin was initially identified in the Rel pathway (Lin et al., 2000), TgCactin localizes to the nucleus, and the Y661H mutation results in a temperature sensitive G1 arrest, we reasoned that TgCactin could be involved in regulation of gene expression. We collected genome-wide expression profile data from the parent and mutant lines at both 35°C and 40°C using the *Toxoplasma* Affymetrix gene chip (Bahl et al., 2010). The gene chip includes 8,058 *T. gondii* genes, of which 5,754 are expressed under the intracellular, extracellular, bradyzoite, or 35°C and 40°C conditions tested. Of these genes 875 are different by a factor of two, either upregulated or downregulated, between intracellular and extracellular tachyzoite wild type parasites (Lescault et al., 2010). For the FV-P6 mutant 138 genes were identified that vary by at least a factor of two when grown at 35°C or 40°C (Fig. 3A,B). Moreover, 43 of the 138 differentially expressed genes are included in the 875 genes that vary between intra- and extracellular parasites (Lescault et al., 2010) (Fig. 3A). This enrichment of differentially expressed genes in FV-P6 is significant (P value = 8.5×10^{-7}, hypergeometric distribution). Therefore, although the FV-P6 mutant was growing intracellularly before the arrest was induced at 40°C and RNA was isolated, the expression profile closely resembles extracellular parasites. Of the genes that are differentially regulated between intra- and extracellular parasites, 43 are also differentially regulated between FV-P6 mutant parasites grown at 35°C and those that are grown at 40°C. Of these genes, in both extracellular parasites and FV-P6 mutants grown at 40°C, 30 are upregulated, while 12 are downregulated.

The FV-P6 mutant also exhibits a significant enrichment in bradyzoite expression characteristics. Of the 463 genes differentially regulated between intracellular tachyzoites and bradyzoites, 35 likewise vary in FV-P6 between growth at 35°C and 40°C ($P<3.110^{-10}$, hypergeometric distribution): in both 40°C FV-P6 and bradyzoites, 30 genes are upregulated and 5 are downregulated (Fig. 3A).

Of the 5754 genes expressed under the conditions tested, 1273 (22.1%) are associated with the G1-stage of the cell cycle (Behnke et al., 2010). When comparing the 875 genes that are 2-fold different between intracellular and extracellular tachyzoites, 229 of them (26.2%; $P=2.9*10^{-4}$) are expressed highly in G1 (Fig. 3B). Of the 138 that are different between FV-P6 at 35°C vs 40°C, 53 genes (38.4%; $P=5.0*10^{-6}$) are specific for G1, in line with the observed G1 arrest. However, of the 463 tachyzoite vs. bradyzoite genes, 154 peak in G1 (33.3%: $P=2.6*10^{-9}$), which probably reflects a slow down of cell cycle progression in bradyzoites (i.e. a higher percentage of parasites are in G1 in a random population). Therefore, the G1 signature of FV-P6 could also suggest enhanced bradyzoite differentiation of the mutant. Since high temperature is a routinely used stress factor to induce bradyzoite differentiation, it is possible that the bradyzoite expression signature is due to the 40°C incubation temperature used to induce the FV-P6 phenotype. To address this potential non-specific aspect we also performed expression profiles on the FV-P6 mutant complemented with the TgCactin encoding cosmid and on a wild-type strain that was complemented with a Y661H mutant *TgCactin* allele to create a pseudodiploid line (see Figure S3 for generation and validation of the pseudo-diploid and Figure S4 for genotype validations of other lines used). Only 19 genes are more than 2-fold differentially expressed between growth at 35°C and 40°C in both the cosmid complemented FV-P6 and the pseudodiploid strains of which only 2 overlap with the genes that were differentially expressed between growth at 35°C and 40°C in the FV-P6 mutant. Therefore, the gene profile expression signatures in arrested FV-P6 is caused by the point mutation in TgCactin, and not due to a stress response originating in incubation at 40°C.

Because, it has recently been demonstrated that the major transcriptional regulators in *Plasmodium* and *Toxoplasma* are the Apetala2 (AP2) proteins (Balaji *et al.*, 2005, Behnke et al., 2010, Painter *et al.*, 2011) we also investigated if any of the 68 *Toxoplasma* AP2 genes were dysregulated in the mutant (only 52 AP2 genes were expressed under the conditions tested and compared here). Interestingly, four of the AP2 genes were at least 2-fold upregulated at the restrictive temperature (Fig. 3C). One of these is expressed during cytokinesis whereas another AP2 transcription factor was previously shown to peak at the G1 stage of the cell cycle (Behnke et al., 2010). In addition, consistent with the gene expression profile signatures, two of the AP2 transcription factors were upregulated both in bradyzoites. Furthermore, all four AP2 transcription factors were upregulated in extracellular parasites.

Thus, the expression profile of the FV-P6 mutant grown at the restrictive temperature resembles that of extracellular parasites and bradyzoites. The differential expression of intra- vs. extracellular genes and tachyzoite vs. bradyzoite genes in this mutant could suggest that Cactin plays a role not only in regulating G1 progression but in regulating state and/or stage differentiation as well. Notably, these parasite states are also reflected in the repertoire of AP2 transcription factors upregulated in FV-P6.

TgCactin is present in a protein complex

Since Cactin itself does not contain any recognizable enzyme activity we reasoned that Cactin likely exerts its function by interacting with other proteins. Moreover, there are several lines of evidence in the literature supporting the interaction of Cactin with other proteins (Ewing *et al.*, 2007, Lin et al., 2000, Lehner *et al.*, 2004, Atzei *et al.*, 2010a). To explore whether TgCactin is also present in a complex we performed native blue gel electrophoresis on parasite lysates. Hereto we transfected a HA3 epitope tagged *TgCactin* allele into both wild-type RH parasites and the FV-P6 mutant. The latter was selected by growth restoration at 40°C to demonstrate that HA3-TgCactin is biologically functional. Native blue gel electrophoresis and western blotting demonstrated that HA3-TgCactin migrates at higher molecular weight than would be expected if it migrated as a monomer,

which has a predicted size of 85 kDa (Fig. 4A). Instead a smear with three reasonably defined bands of approximately 275, 360, and 445 kDa can be discerned in both the wild type and the FV-P6 background.

The conserved mid-region and the C-terminal domain are required for TgCactin oligomerization and function

The protein complexes of approximately 275, 360, and 445 kDa observed by native blue electrophoresis could potentially correlate with tri-, tetra-, and pentamers of the 85 kDa TgCactin protein. To test whether TgCactin could interact with itself we cloned *TgCactin* into yeast two-hybrid (YTH) bait and prey plasmids. Upon transformation in yeast, the interaction strength of these constructs was tested using the *LacZ* (lactamase) and *HIS3* (3-aminotriazole: 3-AT) reporters. Yeast grew on the highest concentration of 50 mM 3-AT (Fig. 4C). In addition, the intensity of the α-lactamase product upon conversion of X-α-Gal was as strong for the TgCactin pair as for the control SNF1/SNF4 interaction pair (Fields & Song, 1989) (data not shown).

To dissect the domains involved in TgCactin's self-interaction, in particular the involvement of the conserved C-terminal domain carrying the *ts* mutation, we designed several mutant and deletion constructs (Fig. 4B). These included full-length TgCactin, with and without the Y661H *ts* mutation, an N-terminal deletion including the conserved mid Catin region (ΔN encoding C-terminal aa 368–703), and a clone only encoding the highly conserved C-terminal domain containing Y661 (CTD: amino acids 585–703) (Fig. 4B). The three constructs were again tested for interaction using the *LacZ* and *HIS3* reporters. The mutant allele in combination with a wild type allele results in a 50% reduction in interaction strength whereas no interaction was observed between two mutant alleles (Fig. 4C). Furthermore, no interaction was detected when two ΔN constructs were paired. Therefore, the data suggest that the conserved C-terminal region is required for self-interaction and that the Y661 plays a crucial role in this interaction. Since two ΔN constructs do not interact, this suggests that another domain besides the C-terminal domain is required for self-interaction. Due to its strong conservation the Cactin mid-region is the best candidate domain to support this interaction. These findings are represented in the schematic in Figure 4D. However, these data could also be explained by lower expression levels of deletion clone or of the *ts* allele relative to the full-length wild-type alleles. Therefore, we validated the expression levels in yeast by western blotting. As shown in Supplementary Figure S5, there are no differences in the amount of protein expressed between the three clones tested. As such, the differences in interaction strengths are directly due to the mutations themselves and do not originate in differential protein expression or stability.

To further validate these findings we asked whether the deletion constructs were able to complement mutant FV-P6. We cloned NLS-containing YFP tagged constructs of the ΔN and the CTD and compared them to the complementation capacity of the full-length TgCactin construct. Complementation, defined by growth restoration at 40°C, was only observed for the full-length TgCactin construct and never for the deletion constructs (data not shown). This again supports the N-terminal half is indeed crucial for TgCactin function, even though the *ts* mutation lies in the C-terminus.

Discussion

The temperature sensitive mutant of TgCactin, FV-P6, arrests irreversibly in G1 due to a single point mutation resulting in a Y661H change in the highly conserved C-terminus, which is involved in self-oligomerization. TgCactin likely exerts its function at the level of gene transcriptional control as supported by genome-wide Affymetrix RNA expression profiling which also identified an additional role in stage differentiation and state switching.

The arrest of FV-P6 is intriguing as the rate at which different apicomplexan parasite strains progress through G1 has been identified as a major factor in the virulence of a particular strain (Gubbels *et al.*, 2008b, Reilly *et al.*, 2007) and may also be a key to drug resistance in the Apicomplexa (Teuscher *et al.*, 2010). Therefore, understanding the requirements for efficient G1 progression could be exploited to develop new therapies that would reduce the impact of apicomplexan diseases. In the case of *Toxoplasma*, checkpoints in the G1 stage of the tachyzoite have been identified by reversible drug blocks using either PDTC (Conde de Felipe et al., 2008), 3-MA (Wang *et al.*, 2010), or by using thymidine parasites overexpressing herpes simplex thymidine kinase (Radke & White, 1998). In addition, a genetic screen for tachyzoite growth mutants identified over a dozen G1 mutants (Gubbels et al., 2008a). However, only two mutants displayed a reversible block, indicating that there is more than one mechanism to arrest in G1. The reversible mutants likely represent defects in the factors involved in the actual G1 block or arrest mechanism, whereas the non-reversible mutants are more likely to have defects in general processes needed to progress through G1. Since mutant FV-P6 is not reversible (Fig. 1E,F) it is unlikely that TgCactin is involved in a cell cycle checkpoint and hence is involved in other processes required for G1 progression. Furthermore, we showed that the mutant arrests at around the midpoint of G1 using dynamic IMC protein markers characteristic of different stages within G1. This arrest is the same for parasites coming out of G0 (upon direct invasion at 40°C) as it is for parasites coming out of cell division (upon replicating first at 35°C). Since the morphology of the arrested parasites is indistinguishable from wild type parasites it is unlikely the arrest is due to structural defects.

A single point mutation resulting in a Y661H substitution in the highly conserved C-terminal domain accounts for the G1 arrest (Fig. 2 and S2). Although the strong conservation of Cactin throughout the eukaryotic lineage suggests a conserved function, the cellular function of Cactin depends to some extent on the species studied. For example, Cactin was originally identified as a factor in the Rel pathway of signal transduction (Lin et al., 2000). It was recently shown that human Cactin (hCactin) also works on the Rel pathway through co-immunoprecipitation with I-kappa-BL (IκBL), which results in the repression of Toll-like receptors and interferon regulator factors (Atzei *et al.*, 2010b), and is a function also observed in *C. elegans* (Pujol et al., 2001). Moreover, it was shown that nuclear localization of hCactin is required for this effect (Atzei et al., 2010b). The nuclear localization of TgCactin is consistent with this observation (Fig. 2D,E). However, since many eukaryotes, including *Toxoplasma*, lack the Rel pathway this cannot be the only mechanism through which Cactin exerts its function. Genomic studies in humans have related hCactin to mRNA splicing (Ewing et al., 2007) and repression of RNA polymerase II elongation (Lehner et al., 2004). In the first study hCactin co-immunoprecipitated with RNA binding protein S1 (RNPS1), a protein associated with nucleocytoplasmic shuttling and surveillance as well as mRNA splicing (Ewing et al., 2007). The second study was designed as a yeast two-hybrid screen and hCactin was identified using the negative elongation factor subunit E (NELF-E) as bait, which is also known as RD RNA-binding protein (RDBP). RDBP cooperates with another complex, DRB-sensitive factor (DSIF), to repress transcription elongation by RNA polymerase II (Lehner et al., 2004). Studies in zebrafish (Atzei *et al.*, 2010c) and *C. elegans* (Tannoury *et al.*, 2010) show that Cactin is essential for embryonic development. Therefore, Cactin appears to have multiple functions, which either revolve around control of gene expression or control and processing of RNA.

Given the association of Cactin in general with transcriptional changes we dissected the function of TgCactin by genome wide expression profiling (Fig. 3). As expected we observe a G1 arrest signature in the expression profile. However, we also detected expression of several genes associated with the extracellular parasites as well as with the bradyzoite stage. The expression of extracellular genes is quite striking since the RNA was extracted from

parasites first grown for several division rounds at 35°C before induction of the G1 arrest at 40°C. Therefore these genes must have been actively switched on. In addition, the expression of bradyzoite genes is quite striking given the G1 arrest because differentiation to the bradzyoite stage has been shown to correlate with a prolonged S-phase, or a stage most closely related to a G2 stage (Radke *et al.*, 2003). However, keeping in mind the mutant nature of FV-P6, it is possible that induction of differentiation could be associated with slower cell cycle progression in general (De Champs *et al.*, 1997). The simultaneous dysregulation of the switches to the extracellular and bradyzoite stages was also recently reported in a differentiation mutant study (Lescault et al., 2010). Interestingly, these defects were associated with a tachyzoite-like cell cycle progression under differentiation inducing conditions. It is therefore possible that the signaling pathways between cell cycle progression and stage differentiation are intertwined, which is reflected in the bradyzoite mutants (Lescault et al., 2010) as well as G1 mutant FV-P6.

The expression of the AP2 transcription factors aligns quite well with the observed expression profiles as factors correlating with G1, bradyzoite, and extracellular parasites are expressed in the arrested FV-P6 parasites (Fig. 3). In recent years the AP2 transcription factors have emerged as key factors directly controlling the expression of groups of genes associated with parasite growth and stage differentiation (Balaji *et al.*, 2005, Behnke et al., 2010, Painter *et al.*, 2011). Indeed we observe several G1 specific AP2 transcription factors upregulated in the arrested FV-P6 mutant, but not all G1 specific AP2 factors are upregulated (Fig. 3C). The absence of upregulation of these G1 specific factors (e.g. AP2X-7, AP2VIIa-6, AP2XII-4, and AP2VIII-4) could therefore result in the transcriptional suppression of genes required for G1 progression. However, the understanding of the transcriptional profiles associated with specific AP2 factors is at the moment insufficient to validate such model.

Our data show that upon incubation at 40°C FV-P6 arrests in G1 within one cell cycle (Fig. 1). These fast kinetics suggest that the arrest originates in the misfolding of TgCactin protein already present rather than protein misfolding upon translation at the restrictive temperature. Furthermore, our data suggest that the mutation is involved in TgCactin self-interaction (Fig. 4D). In addition to demonstrating self-interaction by YTH we also demonstrated that within the parasite TgCactin is present in an oligomeric complex (Fig. 4A). The conserved CTD is not enough for self-interaction and neither can the CTD rescue the arrest in mutant FV-P6. This indicates that the N-terminal half of TgCactin must fulfill a critical function as well. Since pairing a mutant allele with a wild-type allele results in a 50% reduction in self-interaction, our model incorporates the conserved mid-region as a putative domain interacting with the CTD.

Given that TgCactin interacts with itself, in combination with the interaction data obtained from human studies (Lehner et al., 2004, Ewing et al., 2007, Atzei et al., 2010a), it is conceivable that TgCactin functions as a scaffolding protein. How TgCactin organizes this in a cell cycle or developmentally regulated fashion is still unclear. Given the nearly constitutive mRNA expression profile of TgCactin throughout tachyzoite development, post-translational modifications of the TgCactin protein, e.g. through cyclin dependent or mitotic kinases (Gubbels et al., 2008b), is the most likely mechanism. Taken together, TgCactin is required for G1 progression whereas expression profile data support an additional role in stage transition. TgCactin most likely exerts its function by modulating transcription or modifying RNA, a model that is consistent with the general, yet limited understanding of Cactin's mechanism of action in other eukaryotes. The focus of future work will be the identification of proteins interacting with Cactin to elucidate its mechanism of action.

Experimental Procedures

Parasites

All parasites used are RH strain derivatives and were grown in confluent human foreskin fibroblast (HFF) cells (Roos *et al.*, 1994). Regular parasites were grown at 37°C whereas *ts* mutants were grown at either 35°C (permissive) of 40°C (restrictive). Parasite transfections and selections using 1 μM pyrimethamine or 20 μM chloramphenicol at 40°C were performed as described previously (Roos et al., 1994). Complementation with PCR products was performed as described previously (Gubbels et al., 2008a). The Ku80 knock-out parasites ($Ku80^{neg}$; kindly provided by (Fox *et al.*, 2009, Huynh & Carruthers, 2009)) were used to attempt swapping the wild type Cactin allele for the Y661H encoding mutant cDNA allele.

Plasmid constructs

All primer sequences are provided in Supplementary Table S1. Plasmid pcactin-YFP-Cactin/sagCAT was generated by PCR amplifying the 1.5 kb Cactin promoter in front of the start codon with primers pCactin-F-PmeI and pCactin-R-BglII, and replacing the tubulin promoter in ptub-YFP-Cactin/sagCAT using *Pme*I/*Bgl*II restriction enzymes. Plasmid ptub-HA3-Cactin/sagCAT was generated by inserting the PCR amplified Cactin CDS using primers Cactin-F-XmaI and Cactin-R-RV into plasmid ptub-HA3-/sagCAT (kindly provided by Giel van Dooren and Boris Striepen, U. of Georgia) with *Xma*I and *Eco*RV restriction enzymes.

Plasmid ptub-myc2CactinCD4/sagCAT was generated by PCR amplifying the last 354 bp of the Cactin CDS with primers Cact-CD4-F-Avr and Cactin-R-RV followed by *Avr*II/*Eco*RV insertion into plasmid ptubYFP_2(MCS)/sagCAT (Gubbels et al., 2003). CactinCD4 including the 3′dhfr was then swapped into ptub-myc2MORN1/sagCAT (Lorestani *et al.*, 2010) using Avr*II* and Not*I* enzymes to replace MORN1-3′dhfr.

Plasmid ptub-myc2-Cactin/DHFR was generated by first replacing ptub-tandemCherry in ptub-TandemCherry/DHFR (Gubbels et al, unpublished) with ptub-Myc2CactinCD4 from ptub-myc2CactinCD4/sagCAT using *NsiI*/*Not*I enzymes resulting in plasmid ptub-Myc2CactinCD4/DHFR. CactinCD4 in this plasmid was replaced by the full-length Cactin CDS using *Avr*II/*Not*I enzymes from ptub-YFPCactin/sagCAT.

Plasmid ptub-YFP-NLS-CloneΔN Cactin/sagCAT was generated by PCR amplification of Exons 7–9 of Cactin cDNA with F-AvrII-NLS-NheI-ΔN and Cactin-R-RV, *Avr*II/*Eco*RV digestion, and cloned into ptubYFP_2(MCS)/sagCAT.

Plasmid ptub-YFP-NLS-CactinCD4/sagCAT was generated by replacing ΔNCactin by *Nhe*I/*Eco*RV digestion of the plasmid and insertion of CactinCD4 digested with *Avr*II and *Eco*RV from ptub-myc2CactinCD4/sagCAT.

Plasmids pimc7-CherryRFP-IMC7/sagCAT and pimc14-CherryRFP-IMC14/sagCAT were generated using plasmid ptub-mCherryRFP_2/sagCAT ((Chtanova *et al.*, 2008) kindly provided by Giel van Dooren and Boris Striepen, U. of Georgia) in a 2-step process: endogenous promoters were PCR amplified from genomic DNA and replaced the ptub promoter by *Pme*I/*Bgl*II restriction enzymes. The second mCherry ORF was replaced by PCR amplifying the IMC CDS from cDNA using *Avr*II/*Eco*RV restriction enzymes. Plasmids ptub-Cactin-YFP/sagCAT and ptub-YFP-Cactin/sagCAT were generated by PCR amplification of the TgCactin CDS using primer combinations Cactin-F-Bgl and Cactin-R-Avr, and Cactin-F-Avr and Cactin-R-RV, respectively, and cloned with *Bgl*II/*Avr*II and *Avr*II/*Eco*RV, respectively, into plasmid ptub-YFP_2(MCS)/sagCAT (Gubbels et al., 2003).

All yeast-two hybrid (YTH) constructs were made using Gateway Technology (Invitrogen). In short, full-length wild type Cactin and full-length FV-P6 Cactin were PCR amplified in a two-step PCR with AttB1-F-Cactin and AttB2-R-Cactin primers in the first round and universal AttB adapter primers Att-B1-adopt and Att-B2-adopt in the second round. The amplicons were cloned by BP recombination into the pDONR201 vector. Subsequently the inserts were transferred into plasmids pGBK-Att or pGAD-Att vectors by LR recombination. Plasmids pGBK-Att and pGAD-Att were derived from pGBKT7 and pGADT7 plasmids (Clontech), respectively, and converted into Gateway compatible vectors by cloning the reading frame B cassette (Invitrogen) into the *Sma*I site of each plasmid. Cactin ΔN (Exons 7–9 in pGAD-Att) was PCR amplified with AttB1-F-Exon7Cactin and AttB2-R-Cactin and the universal AttB adapter primers and subsequently shuttled into pGBK-Att vector through LR recombination.

PCR-based genotyping

Primer sequences can be found in Supplementary Table S1, and location with TgCactin is shown in Supplementary Figure S3. PCR1 (primers PCR1-F and PCR1-R) can differentiate a genomic DNA allele (with introns: 726 bp) from a cDNA allele (406 bp) PCR2 (primers PCR2-F and PCR1-R) amplifies only genomic DNA (583 bp) whereas PCR3 (primers PCR1-F and PCR3-R) only amplifies alleles wherein the 3′UTR of Cactin is continuous (850 bp). PCR products were Sanger sequenced using primer Cactin-int-seq.

Plaque assays

HFF cells grown to confluence in T12.5 flasks were inoculated with 300 parasites and incubated for 18 hrs at 35°C after which flasks were transferred to 40°C for 0, 8, 16, 24, 32, 40, and 48 hrs and then moved back to the 35°C incubator and left undisturbed for 7 to 11 days. Plaques were stained as described previously (Roos et al., 1994).

Immunofluorescence

Parasite infected HFF cells were methanol fixed as described previously (Anderson-White *et al.*, 2011). The following antibodies were used: mouse 12G10 α-α-tubulin (1:100; Hybridoma Bank, Univ. of Iowa), rabbit α-IMC3 (1:500; (Gubbels et al., 2004)), rabbit α-MORN1 (1:200; (Gubbels et al., 2006)), rabbit α-HsCentrin (1:1000; kindly provided by Iain Cheeseman, Whitehead Institute), and rabbit α-CherryRFP (1:200,000; kindly provided by Iain Cheeseman, Whitehead Institute) in blocking solution. Secondary antibodies were conjugated to Alexa Fluor 488 or Alexa Fluor 594 (Invitrogen) and DNA was stained with 4′,6-diamidino-2-phenylindole (DAPI). Imaging was performed on a Zeiss Axiovert 200M wide-field fluorescence microscope equipped with standard DAPI, FITC, YFP, and TRTC filter sets, a α-Plan-Fluar 100x/1.45 NA oil objective, and a Hamamatsu C4742-95 camera. Images were analyzed and processed using Volocity (Improvision).

Phylogenetic analysis

The accession numbers of the Cactin genes used are: *H. sapiens* (AAH19848), *R. norvegicus* (NP_001074916), *M. musculus* (NP_081657), *D. melanogaster* (NP_523422), *C. elegans* (NP_496951), *A. thaliana* (NP_171887), *T. gondii* (XP_002366927), *E. tenella* (AI757514), *P. knowlesi* (XP_002257640), *P. falciparum* (XP_001349475), *P. yoelii* (XP_727028), *Tetrahymena thermophila* (XP_001024246), *C. parvum* (XP_626113), *L. major* (XP_001684517), *T. brucei* (CBH18183), and *T. cruzi* (XP_810302). Sequences were aligned using the CLUSTAL W algorithm (Thompson et al., 1994) and trees generated in the MegAlign program (DNA Star software) using 1000x bootstrapping.

Sequence analysis of TgCactin

The Pfam database (http://pfam.sanger.ac.uk/; (Finn et al., 2010)) was searched to identify domains within TgCactin. The nuclear localization signal was identified with the NLSdb application available on http://cubic.bioc.columbia.edu/db/NLSdb/ (Nair et al., 2003) as well as with the PSORT (http://psort.hgc.jp/form.html).

Expression array profiling

Parasites were allowed to invade confluent HFF monolayers for 2 hrs at 35°C before the medium was aspirated and the cells washed twice with PBS. Fresh Ed1 medium was added and flasks were left for an additional 16 hrs at 35°C before flasks were either left at 35°C or placed at 40°C and incubated for 24 hrs to induce phenotypic arrest. Parasites were harvested by scraping off the monolayer, needle passing through a 27G needle, and filtration through a 3 μm polycarbonate filter. RNA was extracted using the RNeasy kit (Qiagen) including β-mercaptoethanol and DNase I treatment according to the manufacturer's instructions. RNA quality was determined using the Agilent Bioanalyzer 2100. RNA samples were processed and hybridized at two different facilities: Montana State University and the Massachusetts Institute of Technology. Fragmented cDNA was hybridized to a *T. gondii* Affymetrix Gene Chip (Bahl *et al.*, 2010). Probe intensities were measured with the Affymetrix GeneChip Scanner 3000 7G and were processed into image analysis (.CEL) files with either GeneChip Operating Software or Expression Console Software (Affymetrix). CEL files were processed together with Robust Multi-array Average (RMA) together with CEL files from (Lescault et al., 2010) (GSE23174 record), which contain *Toxoplasma* RH strain gene expression data for intracellular, extracellular and bradyzoite conditions. For extracellular conditions the 11 hr extracellular time-points were used (GEO accession nrs: GSM570474, GSM570475, GSM570476, GSM570477), for intracellular conditions the 24 hr post invasion time-points were used (GSM570420, GSM570421, GSM570422, GSM570423), for bradyzoite conditions the 72 hr induction conditions were used (GSM570424, GSM570425, GSM570426, GSM570427, GSM570428). Differential expression between the FV-P6 mutant at 35°C and 40°C was defined as 2-fold expression difference in the same direction for each of the 2 arrays performed, while differential expression between the other conditions (intracellular vs extracellular, bradyzoite vs tachyzoite) was defined as an average 2-fold difference between the 4–5 arrays for each condition (a value of <6.5 was used as cut-off for background expression and every value below 6.5 was converted to 6.5). To determine if the number of genes that were similarly regulated between two different comparisons was significant we used the hypergeometric distribution. The Venn-diagram was made using BioVenn (Hulsen *et al.*, 2008). All arrays are deposited at the Gene Expression Omnibus (GEO) database under accession numbers GSM893305- GSM893312 (project accession number GSE36432).

Native blue electrophoresis

5×10^8 freshly lysed parasites were filtered through a 3 μm polycarbonate filter, pelleted for 20 min at 1500 × g at 4°C and washed twice with 5 ml PBS. The samples were processed according to the manufacturer's instructions for the Native PAGE Novex Bis-Tris gel system (Invitrogen). In short, parasites were resuspended in 200 μl lysis buffer (150 mM NaCl, 50 mM Tris-Cl pH 7.5, containing 1% Digitonin and mammalian proteinase inhibitors (Sigma P8340)), passed through a 27G needle, and subjected to 5 min mild sonication in a water bath at 4°C. Subsequently, the samples were treated with benzonase (0.01 U/μl) in the presence of 2 mM $MgCl_2$ for 30 min at room temperature. Samples were cleared by centrifugation for 30 min at 4°C at 13,000 rpm in a mini-centrifuge and the 30 μl sample was mixed with 10 μl 4x Native PAGE sample buffer and 0.5 μl of Native PAGE 5% Coomassie G-250 sample additive prior to loading on a 4–16% gradient Native PAGE Novex Bis-Tris gel. The inner chamber of the gel system was filled with Dark Blue cathode

buffer and the outer chamber with Native PAGE running buffer. The samples were run until the dye front migrated through one third of the gel length. Then inner chamber buffer was replaced with Light Blue cathode buffer and the gel was run until the dye front reached the bottom of the gel. Proteins were blotted to polyvinylidene fluoride (PVDF) membrane in NuPAGE transfer buffer. Post-transfer the membrane was treated with 8% acetic acid for 15 min.

Yeast two-hybrid

Saccharomyces cerevisiae strain AH109 (MATa, trp1-901, leu2-3, 112, ura3-52, lys2-181, his3-200, ade2-101, gal4-952, gal80-538, LYS2::GAL1uas-GAL1tata-HIS3, GAL2uas-GAL2tata-ADE2, URA3::MEL1uas-MEL1tata-lacZ) (Clontech) was used. Yeast was transformed using the $LiC_2H_3O_2$ method with either 2.5 μg bait plasmid mixed with 2.5μg of pGAD-Cactin-AD prey plasmid.

Transformed yeast were plated on SD/Trp^-/Leu^- plates and incubated at 30°C until appearance of colonies. Plates were then replica-plated to a quadruple-dropout selective medium (QDO) (SD/His^-/Ade^-/Trp^-/Leu^-). Growing colonies were patched onto new QDO plates, which were subsequently replica plated to QDO/X-α-Gal and QDO/3-aminotriazole (3-AT) at 5, 10, 25, and 50 mM.

Supplementary Material

Refer to Web version on PubMed Central for supplementary material.

Acknowledgments

We would like to thank Iain Cheeseman for sharing antisera, David Bzik and Vern Carruthers for sharing the $Ku80^{neg}$ line, F. Douglas Ivey for expertise with the YTH work, Michael Behnke for technical assistance with the expression profiles, and the MIT BioMicro center for technical assistance with microarrays. This work was funded by a March of Dimes Basil O'Connor Starter Scholar Research Award (5-FY09-08) to MJG and National Institutes of Health grants R01-AI081924 (MJG) R01-AI077662 (MW), R01-AI089885 (MW), and R01-AI080621 (JPJS).

References

Anderson-White BR, Ivey FD, Cheng K, Szatanek T, Lorestani A, Beckers CJ, Ferguson DJP, Sahoo N, Gubbels MJ. A family of intermediate filament-like proteins is sequentially assembled into the cytoskeletal scaffold of Toxoplasma gondii. Cell Microbiol. 2011; 13:18–31. [PubMed: 20698859]

Atzei P, Gargan S, Curran N, Moynagh PN. Cactin targets the MHC class III protein I{kappa}B like (I{kappa}BL) and inhibits NF-{kappa}b and IRF signalling pathways. J Biol Chem. 2010a; 285:36804–36817. [PubMed: 20829348]

Atzei P, Gargan S, Curran N, Moynagh PN. Cactin targets the MHC class III protein I{kappa}B like (I{kappa}BL) and inhibits NF-{kappa}b and IRF signalling pathways. J Biol Chem. 2010b

Atzei P, Yang F, Collery R, Kennedy BN, Moynagh PN. Characterisation of expression patterns and functional role of Cactin in early zebrafish development. Gene Expr Patterns. 2010c; 10:199–206. [PubMed: 20348034]

Bahl A, Davis PH, Behnke M, Dzierszinski F, Jagalur M, Chen F, Shanmugam D, White MW, Kulp D, Roos DS. A novel multifunctional oligonucleotide microarray for Toxoplasma gondii. BMC Genomics. 2010; 11:603. [PubMed: 20974003]

Balaji S, Babu MM, Iyer LM, Aravind L. Discovery of the principal specific transcription factors of Apicomplexa and their implication for the evolution of the AP2-integrase DNA binding domains. Nucleic Acids Res. 2005; 33:3994–4006. [PubMed: 16040597]

Behnke MS, Wootton JC, Lehmann MM, Radke JB, Lucas O, Nawas J, Sibley LD, White MW. Coordinated Progression through Two Subtranscriptomes Underlies the Tachyzoite Cycle of Toxoplasma gondii. PLoS ONE. 2010; 5:e12354. [PubMed: 20865045]

Chtanova T, Schaeffer M, Han SJ, van Dooren GG, Nollmann M, Herzmark P, Chan SW, Satija H, Camfield K, Aaron H, Striepen B, Robey EA. Dynamics of neutrophil migration in lymph nodes during infection. Immunity. 2008; 29:487–496. [PubMed: 18718768]

Conde de Felipe MM, Lehmann MM, Jerome ME, White MW. Inhibition of Toxoplasma gondii growth by pyrrolidine dithiocarbamate is cell cycle specific and leads to population synchronization. Mol Biochem Parasitol. 2008; 157:22–31. [PubMed: 17976834]

De Champs C, Imbert-Bernard C, Belmeguenai A, Ricard J, Pelloux H, Brambilla E, Ambroise-Thomas P. Toxoplasma gondii: in vivo and in vitro cystogenesis of the virulent RH strain. J Parasitol. 1997; 83:152–155. [PubMed: 9057714]

Ewing RM, Chu P, Elisma F, Li H, Taylor P, Climie S, McBroom-Cerajewski L, Robinson MD, O'Connor L, Li M, Taylor R, Dharsee M, Ho Y, Heilbut A, Moore L, Zhang S, Ornatsky O, Bukhman YV, Ethier M, Sheng Y, Vasilescu J, Abu-Farha M, Lambert JP, Duewel HS, Stewart II, Kuehl B, Hogue K, Colwill K, Gladwish K, Muskat B, Kinach R, Adams SL, Moran MF, Morin GB, Topaloglou T, Figeys D. Large-scale mapping of human protein-protein interactions by mass spectrometry. Mol Syst Biol. 2007; 3:89. [PubMed: 17353931]

Fields S, Song O. A novel genetic system to detect protein-protein interactions. Nature. 1989; 340:245–246. [PubMed: 2547163]

Finn RD, Mistry J, Tate J, Coggill P, Heger A, Pollington JE, Gavin OL, Gunasekaran P, Ceric G, Forslund K, Holm L, Sonnhammer EL, Eddy SR, Bateman A. The Pfam protein families database. Nucleic acids research. 2010; 38:D211–222. [PubMed: 19920124]

Fox BA, Ristuccia JG, Gigley JP, Bzik DJ. Efficient gene replacements in Toxoplasma gondii strains deficient for nonhomologous end-joining. Eukaryot Cell. 2009; 8:520–529. [PubMed: 19218423]

Gaji RY, Behnke MS, Lehmann MM, White MW, Carruthers VB. Cell cycle-dependent, intercellular transmission of Toxoplasma gondii is accompanied by marked changes in parasite gene expression. Mol Microbiol. 2011; 79:192–204. [PubMed: 21166903]

Gubbels MJ, Lehmann M, Muthalagi M, Jerome ME, Brooks CF, Szatanek T, Flynn J, Parrot B, Radke J, Striepen B, White MW. Forward Genetic Analysis of the Apicomplexan Cell Division Cycle in Toxoplasma gondii. PLoS Pathog. 2008a; 4:e36. [PubMed: 18282098]

Gubbels MJ, Li C, Striepen B. High-throughput growth assay for Toxoplasma gondii using yellow fluorescent protein. Antimicrob Agents Chemother. 2003; 47:309–316. [PubMed: 12499207]

Gubbels MJ, Vaishnava S, Boot N, Dubremetz JF, Striepen B. A MORN-repeat protein is a dynamic component of the Toxoplasma gondii cell division apparatus. J Cell Sci. 2006; 119:2236–2245. [PubMed: 16684814]

Gubbels MJ, White M, Szatanek T. The cell cycle and Toxoplasma gondii cell division: Tightly knit or loosely stitched? Int J Parasitol. 2008b; 38:1343–1358. [PubMed: 18703066]

Gubbels MJ, Wieffer M, Striepen B. Fluorescent protein tagging in Toxoplasma gondii: identification of a novel inner membrane complex component conserved among Apicomplexa. Mol Biochem Parasitol. 2004; 137:99–110. [PubMed: 15279956]

Haldar K, Mohandas N. Malaria, erythrocytic infection, and anemia. Hematology Am Soc Hematol Educ Program. 2009:87–93. [PubMed: 20008186]

Hulsen T, de Vlieg J, Alkema W. BioVenn - a web application for the comparison and visualization of biological lists using area-proportional Venn diagrams. BMC Genomics. 2008; 9:488. [PubMed: 18925949]

Huynh MH, Carruthers VB. Tagging of endogenous genes in a Toxoplasma gondii strain lacking Ku80. Eukaryot Cell. 2009; 8:530–539. [PubMed: 19218426]

Lehner B, Semple JI, Brown SE, Counsell D, Campbell RD, Sanderson CM. Analysis of a high-throughput yeast two-hybrid system and its use to predict the function of intracellular proteins encoded within the human MHC class III region. Genomics. 2004; 83:153–167. [PubMed: 14667819]

Lescault PJ, Thompson AB, Patil V, Lirussi D, Burton A, Margarit J, Bond J, Matrajt M. Genomic data reveal Toxoplasma gondii differentiation mutants are also impaired with respect to switching into a novel extracellular tachyzoite state. PLoS ONE. 2010; 5:e14463. [PubMed: 21209930]

Lin P, Huang LH, Steward R. Cactin, a conserved protein that interacts with the Drosophila IkappaB protein cactus and modulates its function. Mech Dev. 2000; 94:57–65. [PubMed: 10842059]

Lorestani A, Sheiner L, Yang K, Robertson SD, Sahoo N, Brooks CF, Ferguson DJ, Striepen B, Gubbels MJ. A Toxoplasma MORN1 Null Mutant Undergoes Repeated Divisions but Is Defective in Basal Assembly, Apicoplast Division and Cytokinesis. PLoS ONE. 2010:5.

Mehlhorn H, Shein E. The piroplasms: life cycle and sexual stages. Adv Parasitol. 1984; 23:37–103. [PubMed: 6442536]

Montoya JG, Liesenfeld O. Toxoplasmosis. Lancet. 2004; 363:1965–1976. [PubMed: 15194258]

Nair R, Carter P, Rost B. NLSdb: database of nuclear localization signals. Nucleic acids research. 2003; 31:397–399. [PubMed: 12520032]

Nishi M, Hu K, Murray JM, Roos DS. Organellar dynamics during the cell cycle of Toxoplasma gondii. J Cell Sci. 2008; 121:1559–1568. [PubMed: 18411248]

Painter HJ, Campbell TL, Llinas M. The Apicomplexan AP2 family: integral factors regulating Plasmodium development. Mol Biochem Parasitol. 2011; 176:1–7. [PubMed: 21126543]

Pujol N, Link EM, Liu LX, Kurz CL, Alloing G, Tan MW, Ray KP, Solari R, Johnson CD, Ewbank JJ. A reverse genetic analysis of components of the Toll signaling pathway in Caenorhabditis elegans. Curr Biol. 2001; 11:809–821. [PubMed: 11516642]

Radke JR, Guerini MN, Jerome M, White MW. A change in the premitotic period of the cell cycle is associated with bradyzoite differentiation in Toxoplasma gondii. Mol Biochem Parasitol. 2003; 131:119–127. [PubMed: 14511810]

Radke JR, Striepen B, Guerini MN, Jerome ME, Roos DS, White MW. Defining the cell cycle for the tachyzoite stage of Toxoplasma gondii. Mol Biochem Parasitol. 2001; 115:165–175. [PubMed: 11420103]

Radke JR, White MW. A cell cycle model for the tachyzoite of Toxoplasma gondii using the Herpes simplex virus thymidine kinase. Mol Biochem Parasitol. 1998; 94:237–247. [PubMed: 9747974]

Reilly HB, Wang H, Steuter JA, Marx AM, Ferdig MT. Quantitative dissection of clone-specific growth rates in cultured malaria parasites. Int J Parasitol. 2007; 37:1599–1607. [PubMed: 17585919]

Robbins J, Dilworth SM, Laskey RA, Dingwall C. Two interdependent basic domains in nucleoplasmin nuclear targeting sequence: identification of a class of bipartite nuclear targeting sequence. Cell. 1991; 64:615–623. [PubMed: 1991323]

Roos DS, Donald RG, Morrissette NS, Moulton AL. Molecular tools for genetic dissection of the protozoan parasite Toxoplasma gondii. Methods Cell Biol. 1994; 45:27–63. [PubMed: 7707991]

Shirley MW, Smith AL, Tomley FM. The biology of avian Eimeria with an emphasis on their control by vaccination. Adv Parasitol. 2005; 60:285–330. [PubMed: 16230106]

Tannoury H, Rodriguez V, Kovacevic I, Ibourk M, Lee M, Cram EJ. CACN-1/Cactin interacts genetically with MIG-2 GTPase signaling to control distal tip cell migration in C. elegans. Dev Biol. 2010; 341:176–185. [PubMed: 20188721]

Teuscher F, Gatton ML, Chen N, Peters J, Kyle DE, Cheng Q. Artemisinin-induced dormancy in plasmodium falciparum: duration, recovery rates, and implications in treatment failure. The Journal of infectious diseases. 2010; 202:1362–1368. [PubMed: 20863228]

Thompson JD, Higgins DG, Gibson TJ. CLUSTAL W: improving the sensitivity of progressive multiple sequence alignment through sequence weighting, position-specific gap penalties and weight matrix choice. Nucleic acids research. 1994; 22:4673–4680. [PubMed: 7984417]

Tzipori S, Ward H. Cryptosporidiosis: biology, pathogenesis and disease. Microbes Infect. 2002; 4:1047–1058. [PubMed: 12191655]

Wang Y, Karnataki A, Parsons M, Weiss LM, Orlofsky A. 3-Methyladenine blocks Toxoplasma gondii division prior to centrosome replication. Mol Biochem Parasitol. 2010; 173:142–153. [PubMed: 20609430]

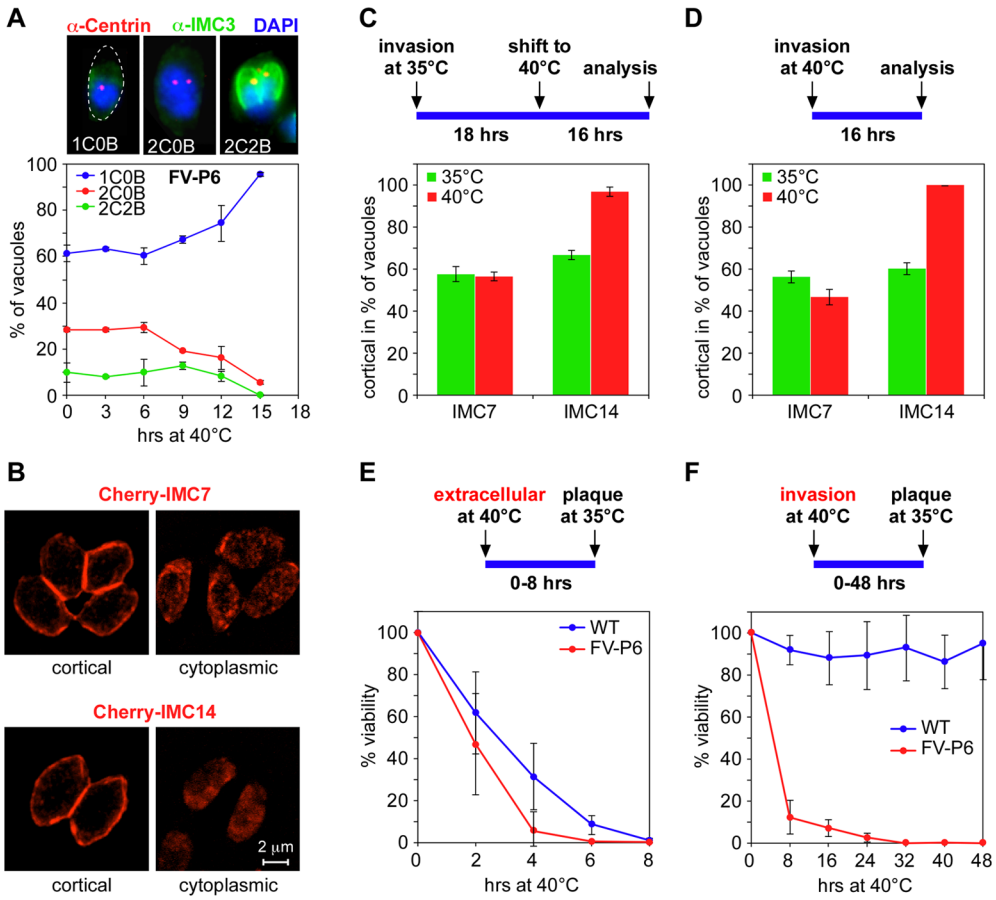

Figure 1. Mutant FV-P6 irreversibly arrests early in G1

A FV-P6 arrests before centrosome duplication and daughter formation. Upper panels: three tachyzoite developmental stages were differentiated by IFA using α-Centrin and α-IMC3 antibodies and by counting the number of centrosomes (1C or 2C) and daughter buds (0B or 2B). Lower panel: quantification of data in A of parasites first grown for 18 hrs at 35°C and then induced for 0–18 hrs in 3 hr intervals at 40°C. **B.** Pictures of parasites expressing mCherry-IMC7 (top panels) or mCherry-IMC14 (lower panels) showing cytoplasmic RFP signal (right panels) or cortical RFP localization (left panels). **C.** FV-P6 expressing mCherry-IMC7 or mCherry-IMC14 were allowed to replicate for 18 hrs at 35°C before transition to 40°C (controls were kept at 35°C). After 16 hrs the localization of IMC7 and IMC14 was differentiated between cytoplasm or cortex. The percentage of vacuoles with cortical signals are plotted for the conditions as indicated (see also supplementary figure S1). **D.** As in panel C except that the parasites were allowed to invade and grow at 40°C for 16 hrs. (All parasites arrest before division). **E.** Freshly lysed wild-type and FV-P6 parasites were incubated for 0–8 hrs at 40°C and then allowed to plaque for 9 days at 35°C. Plaque counts are expressed relative to 0 hrs incubation at 40°C. **F.** As in panel E except that parasites were incubated for 0–48 hrs in the presence of host cells to allow invasion at 40°C. For all graphs averages +/− SD of three independent experiments are shown.

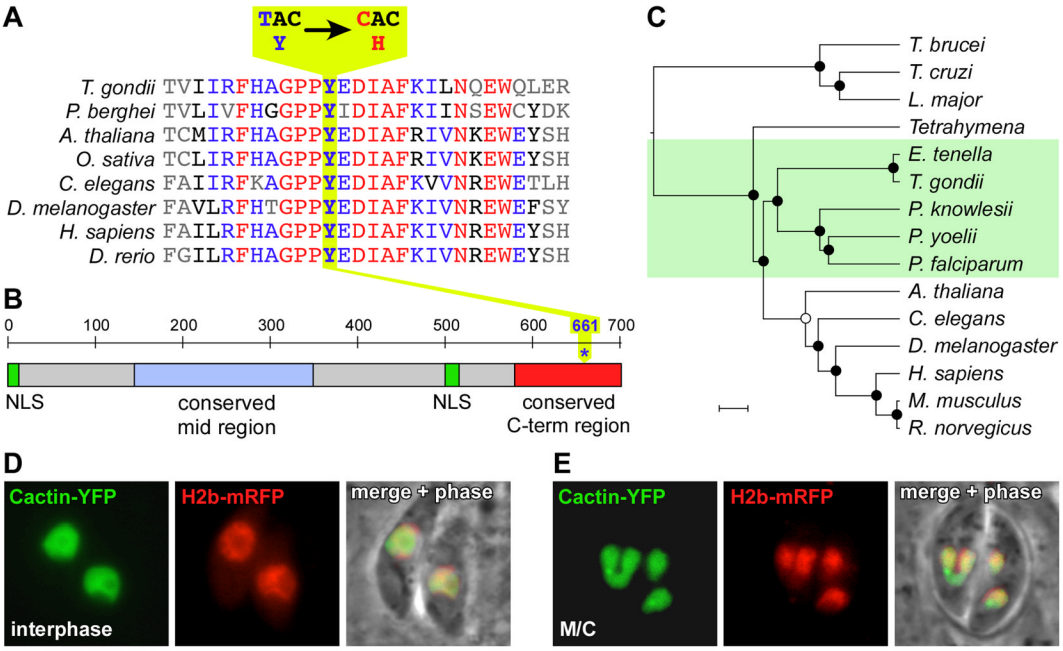

Figure 2. Cactin is conserved across eukaryotes, localizes to the nucleus, and the *ts* mutation results in a tyrosine to histidine change in the conserved C-terminal domain

A. Sequencing of wild-type and FV-P6 *Cactin* alleles identified a single point mutation (T->C) resulting in a Y->H amino acid change. The Y residue is conserved across eukaryotes. **B.** Schematic representation of the TgCactin gene. The N-terminal nuclear localization signal (NLS; aa 3–7: KKRRK), the conserved Cactin mid region and the strongly conserved C-terminal region containing the Y661H mutation are shown. **C.** Phylogenetic analysis identifies an apicomplexan clade (green block). Nodes marked with a solid circle are supported with over 50 bootstrap values; open have less than 50 bootstrap values (1000x bootstrapping). Scale bar represents 20 amino acid changes. **D, E.** Expression of C-terminally YFP-tagged wild type Cactin co-localizes with H2b-mRFP in the nucleus in both G1 (interphase: D) and during mitosis/cytokinesis (M/C: E).

A

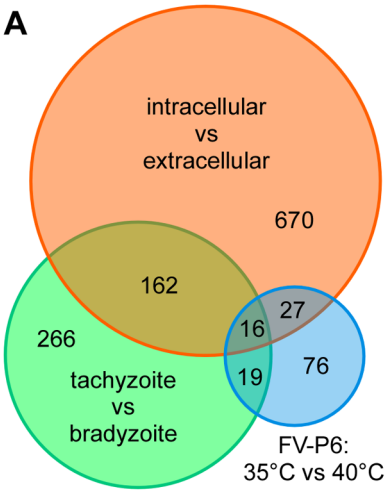

B

condition	total diff. genes	of which G1 expressed (%)	P-value
FV-P6:			
35°C vs 40°C	138	53 (38.4)	$5.0*10^{-6}$
wild type:			
extra vs intra	875	229 (26.2)	$2.9*10^{-4}$
brady vs tachy	463	154 (33.3)	$2.6*10^{-9}$

C

AP2 name	ToxoDB ID TGME49_	stage	fold up
AP2XII-8	050800	C/G1,extra	3.1
AP2VIII-7	069010	G1, extra	4.1
AP2IX-2	064590	brady, extra	2.6
AP2Ib-1	008020	brady, extra	3.0

Figure 3. Gene expression profile of FV-P6 overlaps with extracellular parasites and bradyzoites and has a G1 arrest signature

A. Genes differentially expressed by more than a factor of 2 were identified by genome-wide Affymetrix RNA expression profiles of mutant FV-P6 grown at 35°C and 40°C. Data were compared to 2-fold differentially expressed genes between tachyzoites and bradyzoites as well as to 2-fold differentially expressed genes between intracellular and extracellular tachyzoites (Lescault et al., 2010). The numbers in the Venn diagram represent the number of genes shared between the gene pools. **B.** Number of genes expressed in G1 found in the three different data sets as indicated. The statistical relevance of the enrichment is reflected by the P-value. **C.** Overview of AP2 transcription factors expression levels with a more than 2-fold difference in FV-P6 (averages over two biological replicates are shown). Peak expression in the cell cycle stages (C = cytokinesis; G1), or different development stages ("extra" indicates differential expression between intra- and extra-cellular parasites; "brady" indicates expression in bradyzoites) is indicated

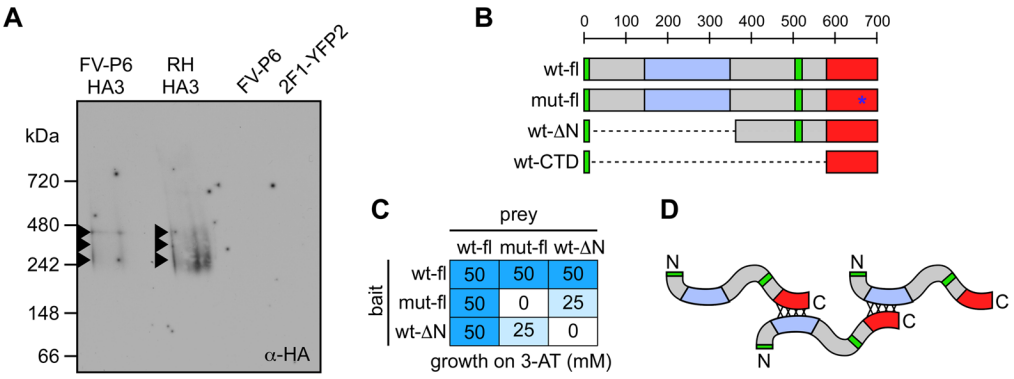

Figure 4. TgCactin forms a multi-meric complex and the ts-mutation in the C-terminal half is involved in self-interaction

A. Native blue gels on FV-P6 mutant or wild type (RH) parasites expressing N-terminally, HA3-tagged TgCactin as indicated. Arrowheads mark the three more discrete protein complexes observed. **B.** Schematic representation of the TgCactin constructs tested by YTH for self-interactions and FV-P6 complementation. For FV-P6 complementation a NLS was added to the wtΔN and C-terminal domain (wt-CTD) constructs in the *Toxoplasma* expression plasmids (absent in YTH plasmids). The asterisk represents the *ts* point mutation. "wt" represents wild-type; "mut" represents the FV-P6 mutant allele; "fl" signifies full-length. Domain color scheme as in Figure 2B. **C.** YTH results of TgCactin interactions with itself. Numbers in the table represent the concentration of 3-AT supporting growth. Blue color represents relative intensity of X-α-Gal staining. **D.** Model of putative TgCactin oligomerization. Domain color scheme as in Figure 2B.